Advances in Concrete Construction, *Vol. 1, No. 4 (2013) 319-340*
DOI: http://dx.doi.org/10.12989/acc2013.1.4.319

Analytical methods for determination of double-*K* fracture parameters of concrete

Shailendra Kumar[*1], Shashi Ranjan Pandey[2a] and A.K.L. Srivastava[2b]

[1]Department of Civil Engineering, Institute of Technology, Guru Ghasidas Vishwavidyalaya, Central University, Bilaspur (C.G.) - 495009, India.
[2]Department of Civil Engineering, National Institute of Technology, Jamshedpur-831014, Jharkhand, India

(Received July 6, 2013, Revised December 3, 2013, Accepted December 10, 2013)

Abstract. This paper presents a comparative study on the double-*K* fracture parameters of concrete obtained using four existing analytical methods such as Gauss–Chebyshev integral method, simplified Green's function method, weight function method and simplified equivalent cohesive force method. Two specimen geometries: three point bend test and compact tension specimen for sizes 100-500 mm at initial notch length to depth ratios 0.25 and 0.4 are used for the comparative study. The required input parameters for determining the double-*K* fracture parameters are derived from the developed fictitious crack model. It is found that the cohesive toughness and initial cracking toughness determined using weight function method and simplified equivalent cohesive force method agree well with those obtained using Gauss–Chebyshev integral method whereas these fracture parameters determined using simplified Green's function method deviates more than by 11% and 20% respectively as compared with those obtained using Gauss–Chebyshev integral method. It is also shown that all the fracture parameters related with double-*K* model are size dependent.

Keywords: three-point bend test; compact tension test; analytical method; double-*K* fracture parameters; weight function; cohesive stress

1. Introduction

The concept of linear elastic fracture mechanics (LEFM) was first applied by Kaplan (1961) to concrete notched beam in order to determine the critical stress intensity factor of concrete. Since 1960s, extensive experimental and numerical investigations on concrete fracture behavior have been carried out by many researchers and it has been observed from past studies that when fracture toughness calculated using the measured values of the maximum load and the initial notch length depends on the dimensions of the test specimens. This size effect of the single parameter based on

LEFM criterion can be attributed mainly to the nonlinear effects associated with crack propagation in concrete. It is well understood that before the development of unstable crack, due to the aggregate interlocking property, there exists a sizeable fracture process zone ahead of initial

∗Corresponding author, Professor, E-mail: shailendrakmr@yahoo.co.in
[a]Associate Professor
[b]Professor

http://www.techno-press.org/?journal=acc&subpage=7 ISSN:2287-5301(Print) 2287-531X(Online)

crack tip, which is primarily responsible for the size effect behavior. In metallic structures, the non-linear behavior results from the strain hardening and plasticity characteristics of the material mainly due to the formation of dislocations whereas the major nonlinear behavior of quasibrittle materials like concrete is associated with the fracture process zone resulting from the formation and branching of micro-cracks. While the nonlinear fracture theories have been developed and successfully applied to metals, these theories have been modified for applications to concrete which includes the tension softening property of the material. The tension softening describes the relationships between traction carrying capacity of cracked concrete and crack opening displacement. The nonlinear fracture models applied to concrete structures are: cohesive crack model (CCM) or fictitious crack model (FCM) (Hillerborg *et al*. 1976, Petersson 1981, Carpinteri 1989, Planas and Elices 1991, Zi and Bažant 2003, Roesler *et al*. 2007, Park *et al*. 2008, Zhao *et al*. 2008, Kwon *et al*. 2008, Cusatis and Schaffert 2009, Elices *et al*. 2009, Kumar and Barai 2008b - 2009c) and crack band model (CBM) (Bažant and Oh 1983), two parameter fracture model (TPFM) (Jenq and Shah 1985), size effect model (SEM) (Bažant *et al*. 1986), effective crack model (ECM) (Nallathambi and Karihaloo 1986), KR-curve method based on cohesive force distribution (Xu and Reinhardt 1998, 1999a), double-*K* fracture model (DKFM) (Xu and Reinhardt 1999a-c, Kumar and Barai 2008a, 2009a, 2010a) and double-*G* fracture model (DGFM) (Xu and Zhang 2008). Among these models, fictitious crack model and crack band model are based on numerical approach in which fracture energy is required as one of the input parameters, while for the other models either the analytical or semi-empirical and semi-analytical formulae in the modified form of LEFM are used in the form of stress intensity factor or fracture energy to express the fracture toughness of concrete.

The double-*K* fracture model can describe the three important stages of crack propagation in concrete viz.: crack initiation, stable crack propagation and unstable fracture in concrete. This method does not require closed loop testing system in the laboratory. The application of this method can be made to large size concrete structures like dam, nuclear reactor vessels, and liquid retaining structures where crack initiation may be one of design criterion including final failure condition. The DKFM is characterized by two material parameters: initial cracking toughness K_ICini and unstable fracture toughness K_{IC}^{un}. The initiation toughness is defined as the inherent toughness of the materials, which holds for loading at crack initiation when material behaves elastically and micro cracking is concentrated to a small-scale in the absence of main crack growth. It is directly calculated by knowing the initial cracking load and initial notch length using LEFM formula. The total toughness at the critical condition is known as unstable toughness K_{IC}^{un} which is regarded as one of the material fracture parameters at the onset of the unstable crack propagation. This parameter can be obtained by knowing peak load and corresponding effective crack length using the same LEFM formula. In double-K fracture criterion, the crack tip stress intensity factor K_I is compared with two material characteristics to describe the different stages of failure conditions. According to this fracture criterion: no crack development will take place if, $K_I < K_{IC}^{ini}$; the onset of crack propagation will occur if, $K_I = K_{IC}^{ini}$; stable crack development will take place if, $K_{IC}^{ini} < K_I < K_{IC}^{un}$; critical unstable crack development will occur if, $K_I = K_{IC}^{un}$ and there will be unstable crack development if, $K_I > K_{IC}^{un}$. Extensive numerical and experimental studies (Xu and Reinhardt 1999a-c, Xu and Reinhardt 2000, Zhao and Xu 2002, Zhang *et al*. 2007, Xu and Zhu 2009, Kumar and Barai 2008a, 2009a-b, 2010a-b; Zhang and Xu 2011, Kumar and Pandey 2012, Hu and Lu 2012, Murthy *et al*. 2012, Hu *et al*. 2012) have been carried out in the past for the study of double-*K* fracture parameters of concrete using different tests specimens with wide range of parameters.

Xu and Reinhardt (1999b) developed Gauss–Chebyshev integral method (GCIM) to calculate the double-*K* fracture parameters for three-point bending test (TPBT) geometry of notched concrete beam. This method requires specialized numerical integration because of singularity problem at the integral boundary for determining the value of cohesive toughness K_{IC}^{C}. The same method was extended to determine the double-*K* fracture parameters for compact tension (CT) and wedge splitting tests (WST) specimens (Xu and Reinhardt 1999c). Later, simplified equivalent cohesive force method (SECFM) (Xu and Reinhardt 2000) was proposed using two empirical formulae to obtain the double-*K* fracture parameters for TPBT configuration. Kumar and Barai (2008a, 2009a, 2010a) introduced the weight function method (WFM) which facilitated a closed form accurate solution for calculating the cohesive toughness of material. Zhang and Xu (2011) presented a simplified Green's function method (SGFM) for determining cohesive toughness of concrete in terms of a closed form solution. Based on fracture tests, the authors (Zhang and Xu 2011) presented a comprehensive comparison of double-*K* fracture toughness parameters of concrete obtained using experimental method and the four existing analytical methods such as: Gauss–Chebyshev integral method (GCIM), simplified Green's function method (SGFM), weight function method (WFM) and simplified equivalent cohesive force method (SECFM). From the study it was presented that the four available analytical methods yield almost the same values of double-*K* fracture toughness parameters and agree well with those obtained from the experimental method.

The main difference between the Gauss–Chebyshev integral method and the simplified equivalent cohesive force method is with respect to the evaluation effective crack extension and cohesive toughness. In the Gauss–Chebyshev integral method, the critical value of effective crack extension is determined using LEFM compliance calibration formula whereas in simplified equivalent cohesive force method it is determined using an empirical expression. In addition, an empirical relation is also used to obtain the value of cohesive toughness in simplified equivalent cohesive force method while a special numerical technique is applied in Gauss–Chebyshev integral method. This numerical integration technique requires more skills because of existence of singularity problem at the integral boundary. In those circumstances, the use of weight function method and simplified Green's function method will provide a closed form expression in determining the value of cohesive toughness.

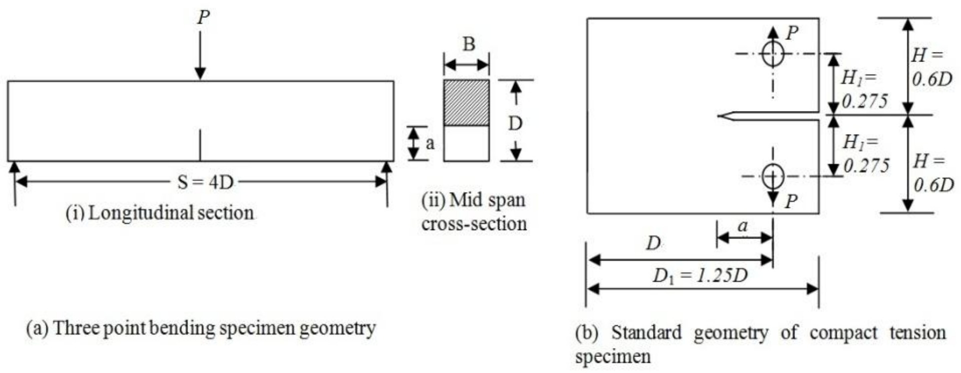

Fig. 1 Three-point bending test and compact tension test Specimens

Based on numerical results, Kumar and Barai (2008a) put forward a similar comparative study on the double-*K* fracture parameters obtained using the then three existing methods such as Gauss–Chebyshev integral method (GCIM), weight function method (WFM) and simplified equivalent cohesive force method (SECFM). Further, using fracture tests, the authors (Zhang and Xu 2011) presented a comparison of double-*K* fracture parameters of concrete obtained using experimental method and the four existing analytical methods i.e., Gauss–Chebyshev integral method (GCIM), simplified Green's function method (SGFM), weight function method (WFM) and simplified equivalent cohesive force method (SECFM). A supplementary contribution on the comparative study of the double-*K* fracture parameters obtained using all the four existing analytical methods employing numerical results may be useful to the interested readers. In view of the above, this paper presents the application of existing four analytical methods to determine the cohesive toughness and hence the double-*K* fracture parameters for two specimen geometries i.e., three point bend test and compact tension test for characteristic dimension sizes 100-500 mm with initial crack length to depth ratios of 0.25 and 0.4. The input data required for obtaining the double-*K* fracture parameters are precisely derived from the developed fictitious crack model. Finally, a systemic numerical study for on comparison of fracture parameters obtained using these methods is carried out. To this end, a brief introduction of the four analytical methods for determination of double -*K* fracture parameters is presented in the subsequent sections.

2. Specimen geometry

Two types of specimen geometries: three-point bending test and compact tension test are considered in the present study for comparative study. RILEM Technical Committee 50-FMC (1985) has recommended the guidelines for determination of fracture energy of cementitous materials using standard three-point bend test on notched beam. The ASTM standard E399-06 (2006) has specified the general proportion and standard configuration for compact tension test. The standard dimensions of the three-point bend test (TPBT) and compact tension (CT) test geometries are shown in Fig. 1.

The symbols: B, D and S are the width, depth and span respectively for TPBT geometry with S/D = 4. The dimensions and configuration of standard CT specimen according to the ASTM standard E399-06 (2006) are: D_1 = 1.25D, H = 0.6D and H_1 = 0.275D.

3. Introduction of double- *K* fracture parameters

The double-*K* fracture parameters can be determined using experimental test results in which the primary requirement is to measure the initial cracking load P_{ini}, initial crack length a_o, peak load P_u and crack mouth opening displacement at peak load $CMOD_c$ from the tests. Generally, two direct methods are employed to determine the value of P_{ini}. In the first method, the P_{ini} is directly obtained during test by means of strain gauges or with the help of acoustic emission or by laser speckle interferometry method at the tip of initial crack tip. In the second method, the starting point of non-linearity in P-CMOD curve obtained from the experiment is considered to be P_{ini}. In this method, proper care should be taken to draw a straight line along the linear part of P-CMOD curve obtained from the test and to locate the distinct bifurcation point between linear and nonlinear parts of the P-CMOD curve. This bifurcation point which is regarded as the initial cracking point yields the value of P_{ini}. Therefore experimental determination of initial cracking load requires high degree of precision and special attention during test. Once, the P_{ini}, a_o, P_u and $CMOD_c$ are recorded, the initial cracking toughness K_{IC}^{ini} and unstable fracture toughness are determined using LEFM equations.

In order to apply LEFM equations for calculating the double-*K* fracture parameters, Xu and Reinhardt (1999b) introduced linear asymptotic superposition assumption. The hypotheses of the assumption are given below

1. the nonlinear characteristic of the load-crack mouth opening displacement (P-CMOD) curve is caused by fictitious crack extension in front of a stress-free crack, and
2. an effective crack consists of an equivalent-elastic stress-free crack and equivalent-elastic fictitious crack extension.

A detailed explanation of the hypotheses may be seen elsewhere (Xu and Reinhardt 1999b).

3.1 Determination of stress intensity factor

3.1.1 For standard TPBT geometry with S/D = 4 using Tada et al. (1985) formulae

For this case, the stress intensity factor is expressed as

$$K_I = \sigma_N \sqrt{D} k(\alpha) \tag{1}$$

$$k(\alpha) = \sqrt{\alpha}\,\frac{1.99 - \alpha(1-\alpha)(2.15 - 3.93\alpha + 2.7\alpha^2)}{(1+2\alpha)(1-\alpha)^{3/2}} \tag{2}$$

Where $k(\alpha)$ is a geometric factor, $\alpha = a/D$ and σ_N is the nominal stress in the beam due to external load P and self weight of the structure which is given by

$$\sigma_N = \frac{3S}{4bD^2}[2P + w_g S] \tag{3}$$

In Eq. (3), w_g is the self weight per unit length of the structure.

3.1.2 For standard CT specimen using ASTM standard E399-06 (2006) formulae

For CT specimen, the stress intensity factor is expressed as

$$K_I = \sigma_N \sqrt{D}\, k(\alpha) \tag{4}$$

$$k(\alpha) = \frac{(2+\alpha)\left[0.886 + 4.64\alpha - 13.32\alpha^2 + 14.72\alpha^3 - 5.6\alpha^4\right]}{(1-\alpha)^{3/2}} \tag{5}$$

Where $\alpha = \dfrac{a}{D}$, $\sigma_N = \dfrac{P}{BD}$ and Eq. (5) is valid for, $0.2 \leq \alpha \leq 1$ within 0.5% accuracy.

Eqs. (1) and (4) can be used in calculation of initial cracking toughness K_{IC}^{ini} at the tip of initial crack length a_o and unstable fracture toughness K_{IC}^{un} at the tip of effective crack length a_c for

TPBT and CT test specimen geometries respectively. This means that the value of $P = P_{ini}$ and $a = a_o$ will be used for determining the initial cracking toughness whereas and $P = P_u$ and $a = a_c$ will be used for evaluating the unstable fracture toughness of material in the above equations. Since it is difficult to detect the crack initiation load from experimental approach, an inverse analytical method is used to calculate the value of K_{IC}^{ini}. Either in experimental method where the value of P_{ini} is obtained from the test or in the analytical method, the value of effective crack extension corresponding to peak load has to be determined using following procedure.

3.2 Effective crack extension

Using linear asymptotic superposition assumption, the equivalent-elastic crack length at maximum load can be determined by solving LEFM formulae for each type of specimen geometry as mentioned below.

3.2.1 For TPBT geometry, S/D = 4 using Tada et al. (1985) formulae

$$CMOD = \frac{6PSa}{BD^2E} V_1(\beta) \tag{6}$$

$$V_1(\beta) = 0.76 - 2.28\beta + 3.87\beta^2 - 2.04\beta^3 + \frac{0.66}{(1-\beta)^2} \tag{7}$$

where $\beta = \frac{(a + H_o)}{(D + H_o)}$; $a = a_c$ equivalent-elastic crack length at maximum load, $P = P_u$, H_o = thickness of the clip gauge holder. The measured initial compliance C_i from the P-CMOD curve is used to calculate the Young's modulus, E as per the RILEM formula (1990).

$$E = \frac{6Sa_o}{C_i bD^2} V_1(\beta_o) \tag{8}$$

In Eq. (8), a_o = initial notch length and $\beta_o = \frac{(a_o + H_o)}{(D + H_o)}$.

3.2.2 For standard CT specimen using Murakami (1987) equations

Similar to Eq. (6), the crack opening displacement for CT specimen is expressed as

$$COD = \frac{P}{BE} V_1(\alpha) \tag{9}$$

$$V_1(\alpha) = \left[2.163 + 12.219\alpha - 20.065\alpha^2 - 0.9925\alpha^3 + 20.609\alpha^4 - 9.9314\alpha^5\right]\left(\frac{1+\alpha}{1-\alpha}\right)^2 \tag{10}$$

where, $\alpha = \dfrac{a}{D}$, $a = a_c$ *i.e.*, equivalent-elastic crack length at maximum load P_u. The empirical Eq. (10) is valid within 0.5% accuracy for, $0.2 \le \alpha \le 0.975$. The value E is calculated using the P-COD curve as

$$E = \frac{V_1(\alpha_o)}{C_i B} \tag{11}$$

Karihaloo and Nallathambi (1991) concluded that almost the same value of E might be obtained form P-CMOD curve, load-deflection curve and compressive cylinder test. Hence, in case initial compliance is not known the value of E determined using compressive cylinder tests may be used to obtain the critical crack length of the specimen.

3.3 Analytical methods for evaluation of K_{IC}^{ini}

According to analytical method, the following relation can be employed to determine the initial cracking toughness of the material.

$$K_{IC}^{ini} = K_{IC}^{un} - K_{IC}^{C} \tag{12}$$

Where, K_{IC}^{C} is known as cohesive toughness of the material. In Eq. (12), the value of K_{IC}^{un} is obtained using experimental data (P_u and $CMOD_c$) as mentioned in the previous section. Once the value of K_{IC}^{C} is determined, the K_{IC}^{ini} can be obtained using Eq. (12). It is a well known phenomenon that in the fracture process zone, a nonlinear stress profile can develop before the peak load depending on type of cohesive laws. Further, the linear stress distribution was considered for loading stage up to the peak load and the corresponding critical effective crack extension a_c for the development of the double-*K* fracture model (Xu and Reinhardt 1999b). This assumption might lead to the simplification in numerical computations without affecting much on the final values of fracture parameters. Moreover, this assumption seems to be reasonable because up to the peak load, the process zone length is relatively small and mainly the initial portion of the softening branch is used. Based on experimental results and analysis, Zhang and Xu (2011) put forward that the linear cohesive stress distribution along fictitious crack is not applicable when the depth of the specimen is more than 600 mm. In the present study, the depth of specimen is limited to 500 mm and therefore linear cohesive stress distribution is adopted in the fictitious fracture zone. The cohesive stress acting in the fictitious fracture zone on three point bend test specimens is idealized as a series of pair normal forces subjected to single edge cracked specimen of finite width as shown in Fig. 2. The linearly varying distribution of cohesive stress in the fracture zone at peak load is presented in Fig. 3.

The value of cohesion toughness K_{IC}^{C} is negative because of closing stress in fictitious crack zone. However, the absolute value of K_{IC}^{C} is taken as a contribution of the total fracture toughness. Four analytical methods: Gauss–Chebyshev integral method (Xu and Reinhardt 1999b,c), simplified equivalent cohesive force method (Xu and Reinhardt 2000), simplified Green's function method (Zhang and Xu 2011) and weight function method (Kumar and Barai 2008a, 2009a, 2010a) can be used to determine the value of K_{IC}^{C} and hence the K_{IC}^{ini}. During loading of specimen, the critical condition is achieved at maximum load value and the corresponding critical crack tip

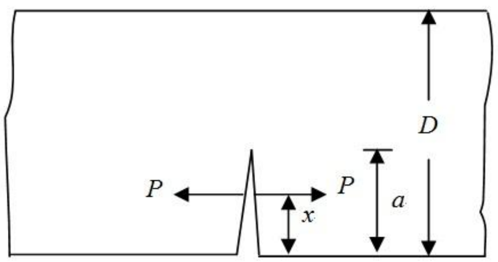

Fig. 2 Single edge cracked specimen of finite width subjected to a pair of normal forces

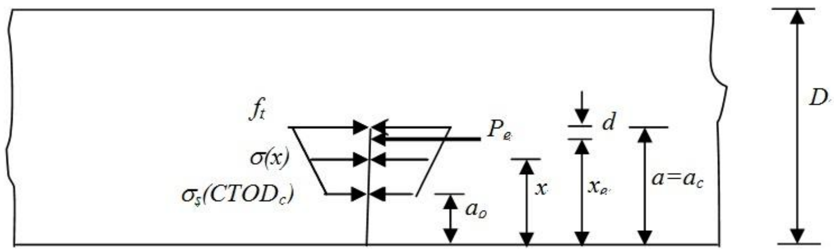

Fig. 3 Distribution of cohesive stress in the fictitious crack zone at critical load

opening displacement (CTOD) is termed as $CTOD_c$. In Fig. 3, the $\sigma_s(CTOD_c)$ is cohesive stress corresponding to $CTOD_c$ at the tip of initial notch, then $\sigma(x)$ is expressed in the following expression.

$$\sigma(x) = \sigma_s(CTOD_c) + \frac{x - a_o}{a - a_o}[f_t - \sigma_s(CTOD_c)] \tag{13}$$

Eq. (13) is expressed in non-dimensional form of crack length, $U = x/a$, as

$$\sigma(U) = \sigma_s(CTOD_c) + \frac{U - a_o/a}{1 - a_o/a}[f_t - \sigma_s(CTOD_c)] \tag{14}$$

Eq. (14) is valid for, $a_o/a \leq U \leq 1$ or $0 \leq CTOD \leq CTOD_c$. The value of $\sigma_s(CTOD_c)$ is calculated by using softening functions of concrete such as bilinear, quasi-exponential, nonlinear, etc. However, in the present work, the nonlinear softening function (Reinhardt *et al*. 1986) is used for all computations which can be expressed as

$$\sigma(w) = f_t\left\{\left[1 + \left(\frac{c_1 w}{w_c}\right)^3\right]\exp\left(\frac{-c_2 w}{w_c}\right) - \frac{w}{w_c}\left(1 + c_1^3\right)\exp\left(-c_2\right)\right\} \tag{15}$$

The value of total fracture energy of concrete G_F is expressed as

$$G_F = w_c f_t \left\{ \frac{1}{c_2}\left[1+6\left(\frac{c_1}{c_2}\right)^3\right] - \left[1+c_1^3\left(1+\frac{3}{c_2}+\frac{6}{c_2^2}+\frac{6}{c_2^3}\right)\right]\frac{\exp(-c_2)}{c_2} - \left(\frac{1+c_1^3}{2}\right)\exp(-c_2)\right\} \quad (16)$$

In which, $\sigma(w)$ is the cohesive stress at crack opening displacement w at the crack-tip and c_1 and c_2 are the material constants. Also, $w = w_c$ for $f_t = 0$, i.e., w_c is the maximum crack opening displacement at the crack-tip at which the cohesive stress becomes to be zero. The value of w_c is computed using Eq. (16) for a given set of values c_1, c_2 and G_F. For normal concrete the values of c_1 and c_2 are taken as 3 and 7 respectively and also these values are used in the present work.

3.4 Determination of $CTOD_c$

It is difficult to measure the value of $CTOD_c$ directly, therefore, for practical purposes the value of crack mouth opening displacement (CMOD) is monitored. At critical condition, the value of crack mouth opening displacement becomes to be critical value of $CMOD_c$ and for the known value of CMOD the crack opening displacement within the crack length, $COD(x)$ is computed using the following expression (Jenq and Shah 1985).

$$COD(x) = CMOD_c \left\{(1-x/a)^2 + (1.081-1.149a/D)[x/a-(x/a)^2]\right\}^{1/2} \quad (17)$$

In Eq. (17), the $CTOD_c = COD(x)$ for $x = a_o$ and $a = a_c$.

3.5 Analytical methods for computation of cohesive toughness

3.5.1 Gauss–Chebyshev integral method

In this method, the stress intensity factor for the case of an edge crack subjected to a pair of normal point forces P acting at a distance x as shown in Fig. 2 is expressed (Tada *et al*. 1985) as

$$K_I = \frac{2P}{\sqrt{\pi a}} F(x/a, a/D) \quad (18)$$

where, $F(x/a, a/D)$ is Green's function and given as

$$F(x/a,a/D) = \frac{3.52(1-x/a)}{(1-a/D)^{3/2}} - \frac{4.35-5.28x/a}{(1-a/D)^{1/2}} + \left\{\frac{1.30-0.30(x/a)^{3/2}}{\sqrt{[1-(x/a)^2]}} + 0.83-1.76x/a\right\} \times [1-(1-x/a)a/D] \quad (19)$$

Putting $U = x/a$ and $\alpha = a/D$ in Eqs. (18) and (19), the final form of integral equation for cohesive toughness due to cohesive stress distribution is expressed as

$$K_{IC}^{C} = \int_{a_o/a}^{1} 2\sqrt{\frac{a}{\pi}}\sigma(U)F(U,\alpha)d\alpha \tag{20}$$

where

$$\begin{aligned} F(U,\alpha) = {} & \frac{3.52(1-U)}{(1-\alpha)^{3/2}} - \frac{4.35-5.28U}{(1-\alpha)^{1/2}} + \\ & \left\{\frac{1.30-0.30U^{3/2}}{\sqrt{[1-U^2]}} + 0.83 - 1.76U\right\}[1-(1-U)\alpha] \end{aligned} \tag{21}$$

At critical condition the value of a is taken to be a_c. The integration of the Eq. (20) is done using Gauss-Chebyshev quadrature method because of existence of singularity at the integral boundary.

3.5.2 Simplified equivalent cohesive force method

According to the simplified equivalent cohesive force method, the evaluation of K_{IC}^{C} is done using a calibration function $Z(x_e/a,\ a_o/a)$ with Eq. (18). The distributed cohesive force $\sigma(x)$ is converted into a single equivalent force P_e per unit thickness as shown in Fig. 3. The absolute value of the K_{IC}^{C} is then expressed as

$$K_{IC}^{C} = Z\left(\frac{x_e}{a},\frac{a_o}{a}\right)\frac{2P_e}{\sqrt{\pi a}}F(x_e/a, a/D) \tag{22}$$

Putting, $U_e = x_e/a$, $\alpha_o = a_o/D$ and $\alpha = a/D$ in Eq. (22), the non-dimensional value of $\frac{K_{IC}^{C}}{f_t\sqrt{D}}$ is expressed as

$$\frac{K_{IC}^{C}}{f_t\sqrt{D}} = Z\left(U_e,\frac{\alpha_o}{\alpha}\right)\frac{2P_e}{f_t\sqrt{\pi a D}}F(U_e,\alpha) \tag{23}$$

For trapezoidal cohesive stress distribution, using a non-dimensional factor γ as

$$\gamma = \frac{\sigma_s(CTOD_c)}{f_t} \tag{24}$$

Then, Eq. (14) can be represented in non-dimensional form as

$$\frac{\sigma(U)}{f_t} = \gamma + \frac{(U-\alpha_o/\alpha)}{(1-\alpha_o/\alpha)}[1-\gamma] \tag{25}$$

From Fig. 3, the value of resultant force P_e can be written as

$$P_e = \frac{f_t}{2}(1+\gamma)(a-a_o) \quad \text{for } a \le a_c \tag{26}$$

In non-dimensional form, Eq. (23) is expressed as

$$\frac{2P_e}{f_t\sqrt{\pi aD}} = (1+\gamma)(1-\alpha_o/\alpha)\sqrt{\alpha/\pi} \tag{27}$$

It is shown in Fig. 3 that d is the centroid of the resultant cohesive force P_e measured from the extending crack tip. Hence d is calculated as

$$d = \frac{(1+2\gamma)}{3(1+\gamma)}(a-a_o) \tag{28}$$

and

$$x_e = a - d = a - \frac{(1+2\gamma)}{3(1+\gamma)}(a-a_o) \tag{29}$$

Also,

$$U_e = \frac{x_e}{a} = \frac{1}{3(1+\gamma)}\left\{2+\gamma+(1+2\gamma)\frac{\alpha_o}{\alpha}\right\} \tag{30}$$

Finally, the calibration function can be empirically determined in the following form.

$$Z(U_e,\alpha_o/\alpha) = \frac{6(1.025-0.1\gamma)}{1+1.83(\alpha_o-0.2)}\left(\frac{\alpha_o}{\alpha}\right)^p\sqrt{\frac{\alpha}{\pi}}U_e^{-0.2} \quad \text{for } 0.2 \le \alpha_o \le 0.8 \tag{31}$$

where,

$p = 1.5(\alpha_o - 0.2) + 0.8$, for $0.2 \le \alpha_o \le 0.6$; $p = 3(\alpha_o - 0.6)+1.4$, for $0.6 \le \alpha_o \le 0.7$ and $p = 6(\alpha_o - 0.7)+1.7$, for $0.7 \le \alpha_o \le 0.8$.

The value of $F(U_e, \alpha)$ in Eq. (23) is computed using Eq. (21), and then the value of K_{IC}^C is obtained using Eqs. (23) and (31).

3.5.3 Simplified Green's function method

In this method, the Green's function $F(x/a, a/D)$ of Eq. (21) can be simplified in the following form

$$F(U,\alpha) = A'U + B' + \frac{1}{\sqrt{1-U^2}} \tag{32}$$

where

$$U = x/a, \alpha = a/D, A' = -\frac{2.23\alpha^2+1.16\alpha+0.17}{(1-\alpha)^{2/3}}, B' = \frac{1.65\alpha^2+1.67\alpha+0.24}{(1-\alpha)^{2/3}}$$

As compared to the Green's function, Eq. (32) yields maximum error of 1% in the entire range of investigation (Zhang and Xu 2011). Hence for linear cohesive stress distribution, the cohesive toughness of the material can be obtained after integrating Eq. (20) in which the value $F(U, \alpha)$ is replaced by Eq. (32). Thus, the value of K_{IC}^{C} is obtained as

$$K_{IC}^{C} = 2\sqrt{\frac{a_c}{\pi}} \int_{\alpha_o/\alpha_c}^{1} \left(k_1 U_c + k_2\right)\left(A' U_c + B' + \frac{1}{\sqrt{1-U_c^2}} \right) dU_c \qquad (33)$$

where, $U_c = x/a_c, \alpha_o = a_o/D, \alpha_c = a_c/D, k_1 = \frac{f_t - \sigma_s(CTOD_c)}{\alpha_c - \alpha_o}\alpha_c, k_2 = \frac{\alpha_c \sigma_s(CTOD_c) - \alpha_o f}{\alpha_c - \alpha_o}$

The values of *A*' and *B*' in Eq. (33) can be obtained by putting $\alpha = \alpha_c$ in Eq. (32). After integration, Eq. (33) yields closed form solution for K_{IC}^{C} as given below.

$$K_{IC}^{C} = 2\sqrt{\frac{a_c}{\pi}} \left[\frac{A'k_1}{3} U_c^3 + \frac{A'k_2 + B'k_1}{2} U_c^2 + B'k_2 U_c - k_1\sqrt{1-U_c^2} + k_2 \arcsin(U_c) \right]_{U_c=\alpha_o/\alpha_c}^{U_c=1} \qquad (34)$$

3.5.4 Weight function method

The weight function method was presented by Kumar and Barai (2008a, 2009a, 2010a). According to this method universal form of weight function having four terms or five terms can be used to express the Green's function. For more accuracy the universal form of weight function with five terms is used in the present study. The universal form of weight function having five terms is expressed as

$$m(x,a) = \frac{2}{\sqrt{2\pi(a-x)}}\left[1 + M_1(1-x/a)^{1/2} + M_2(1-x/a) + M_3(1-x/a)^{3/2} + M_4(1-x/a)^2\right] \qquad (35)$$

In Eq. (35), first of all three parameters M_1, M_2, M_3 and M_4 of five-term universal weight function is determined in which the values of M_1, M_2 M_3 and M_4 can be represented as a function of *a/D* ratio in the following form.

$$M_i = \frac{1}{(1-a/D)^{3/2}}\left[a_i + b_i a/D + c_i(a/D)^2 + d_i(a/D)^3 + e_i(a/D)^4 + f_i(a/D)^5\right] \qquad (36)$$

for, i = 1 and 3 and

$$M_i = \left[a_i + b_i a/D\right] \text{ for } i = 2 \text{ and } 4. \qquad (37)$$

The values of coefficients a_i, b_i, c_i, . . ., f_i are given in Table 1.

From comparison between the Tada Green's function and five terms weight function it has been found that the maximum absolute difference in result is less than 1% for $0.2 < a/D \leq 0.95$ and it is less than 1.5 % for $0 \leq a/D \leq 0.2$ in the range of crack length of $0 \leq x/a \leq 0.98$. Then the stress intensity factor using weight function method can be expressed as

$$K = \int_0^a \sigma(x).m(x,a)dx \qquad (38)$$

Table 1 Coefficients of five terms weight function parameters M_1, M_2, M_3 and M_4

i	a_i	b_i	c_i	d_i	e_i	f_i
1	-0.000824975	0.6878602	0.4942668	-3.25418434	3.4426983	-1.3689673
2	0.782308	-3.0488836				
3	-0.3049218	13.4186519	-23.31662697	35.51066606	-34.440981408	14.10339412
4	0.28347699	-7.378355423				

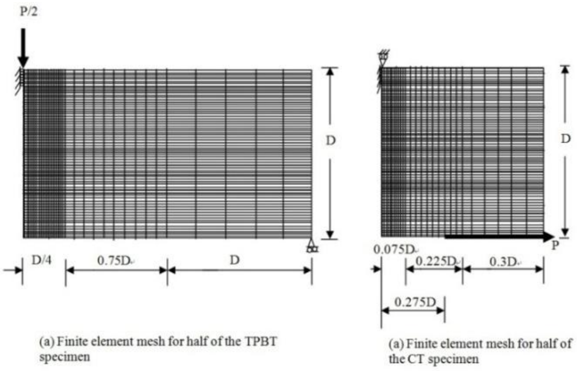

Fig. 4 Finite element discretization of TPBT and CT specimens

The value of $\sigma(x)$ in Eq. (38) is replaced by Eq. (13), hence a closed form expression for K_{IC}^C can be obtained as

$$K_{IC}^C = \frac{2}{\sqrt{2\pi a}}\left\{A_1 a\left[2s^{1/2} + M_1 s + \frac{2}{3}M_2 s^{3/2} + \frac{M_3}{2}s^2 + \frac{2}{5}M_4 s^{5/2}\right] + \right.$$

$$\left. A_2 a^2\left[\frac{4}{3}s^{3/2} + \frac{M_1}{2}s^2 + \frac{4}{15}M_2 s^{5/2} + \frac{4}{35}M_4 s^{7/2} + \frac{M_3}{6}\left\{1-(a_o/a)^3 - 3sa_o/a\right\}\right]\right\} \quad (39)$$

where, $A_1 = \sigma_s(CTOD_c), A_2 = \dfrac{f_t - \sigma_s(CTOD_c)}{a - a_o}$ and $s = (1 - a_o/a)$. At the critical effective crack extension, a is equal to a_c in Eq. (39). After determining the value of K_{IC}^C using any of the above mentioned methods, the value of K_{IC}^{ini} can be evaluated using Eq. (12).

4. Fictitious crack model

The cohesive crack model (CCM) or fictitious crack model (FCM) has been developed and used by many researchers (Petersson 1981, Carpinteri 1989, Planas and Elices 1991, Zi and Bažant 2003, Roesler *et al*. 2007, Park *et al*. 2008, Zhao *et al*. 2008, Kwon *et al*. 2008, Cusatis and Schaffert 2009, Elices *et al*. 2009, Kumar and Barai 2008b, 2009c) in the past for characterizing the softening functions and predicting the nonlinear fracture characteristics of concrete using various test configurations. Three material properties such as modulus of elasticity E, uniaxial tensile strength f_t, and fracture energy GF are required to model FCM or CCM. The concrete mix with material properties: v = 0.18, f_t = 3.21MPa, E = 30 GPa, and G_F = 103N/m along with nonlinear stress-displacement softening relation with constants c_1 = 3 and c_2 = 7 are used as the input parameters in the present study.

The following assumptions are considered in the development of cohesive crack model (Petersson 1981, Carpenteri 1989, Kumar and Barai 2009c): (i) the bulk of material behaves in a linear elastic and isotropic manner, (ii) the fracture process zone begins to develop when the maximum principal stress becomes equal to the tensile strength and (iii) the material is in partial damaged condition and is still able to transfer the stress known as cohesive stress which depends on the crack opening displacement. Also two material lengths (i) the fracture process zone and (ii) the width of the FPZ have always been considered as a matter of research in the fracture modelling of concrete. Petersson (1981) showed experimentally that the size of FPZ is significant and comparable but its width is normally small (in the order of maximum aggregate size) with respect to the characteristic dimension of a structure. In the fictitious crack model, the FPZ is assumed to have collapsed into a line or a surface in two or three-dimensional analysis, respectively. In the pure mode I loading if a single macroscopic crack opens in a fixed direction, the cohesive crack can be modelled easily by adopting procedures proposed by Petersson (1981), Carpinteri (1989) and Planas and Elices (1991). In this method the number of fracture nodes along the potential crack line is kept as fixed in the FEM and only a standard linear finite element analysis is needed to determine the required influence coefficients along the potential crack line. Since away from the potential crack line i.e., the bulk of material behaves in linear elastic manner, even after considering the coarser meshing in this region it will not affect the influence coefficients along the potential crack line. This is the reason why the finer mesh is considered along the potential crack line and coarser mesh is considered in the bulk of specimen. With this background, the present FEM meshing is done which requires relatively less memory in the computer while running the programme. In this method, the governing equation of crack opening displacement (COD) along the potential fracture line is written. The influence coefficients of the COD equation are determined using linear elastic finite element method. Four noded isoparametric plane elements are used in finite element calculation. The COD vector is partitioned according to the enhanced algorithm introduced by Planas and Elices (1991). Finally, the system of nonlinear simultaneous equation is developed and solved using Newton-Raphson method. For standard three point bend test and compact tension test specimens with B = 100 mm having size range D = 100-500 mm, the finite element analysis is carried out for which the half of the specimens are discretized due to symmetry considering 80 numbers of equal isoparametric plane elements along the dimension D. The descritization of both the test geometries is shown in Fig. 4

Due to symmetry, half of the three point bend test and compact tension test specimens are descritized.

5. Results and discussion

The various numerical results as obtained in the present study are plotted in Figs. 5-14. Fig. 5 shows the variation of P_u with specimen size (D) in which it can be seen that the peak load increases with the specimen depth. For given value of D and a_o/D ratio, the peak load capacity of compact tension specimen is more than those of three point bend test specimen.

The value of $CMOD_c$ versus specimen size is plotted in Fig. 6, in which, it is found that the value of $CMOD_c$ increases with the specimen size. Also, for given value of D and a_o/D ratio, the

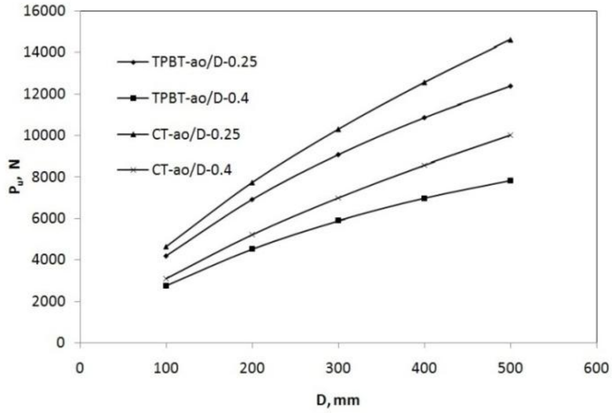

Fig. 5 Variation of peak load with specimen size

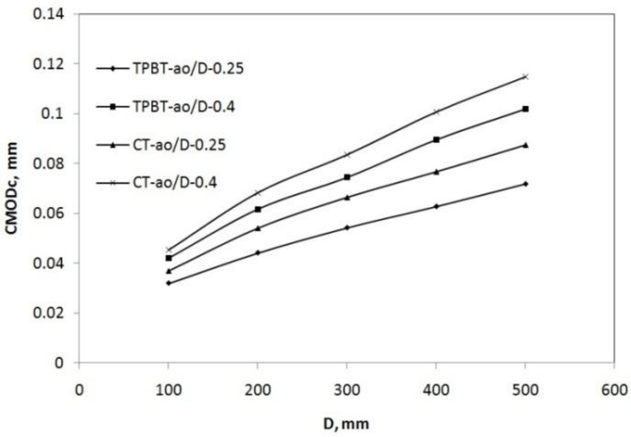

Fig. 6 Variation of CMODc with specimen size

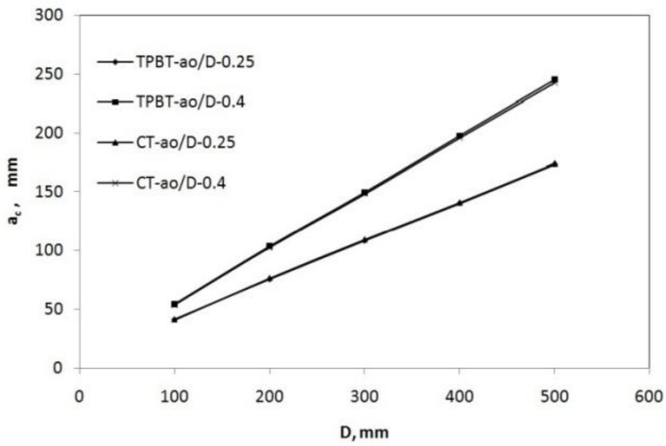

Fig. 7 Variation of critical effective crack extension with specimen size

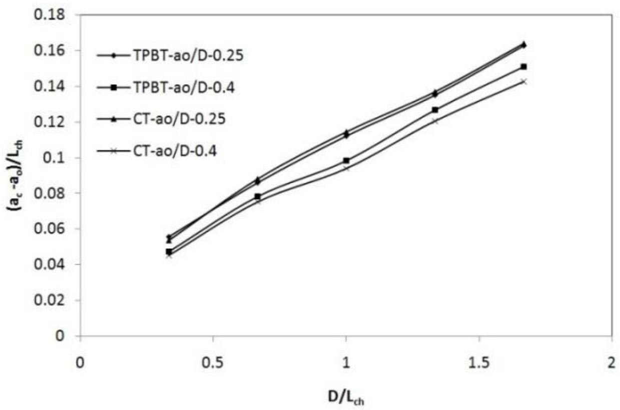

Fig. 8 Variation of critical FPZ with specimen size in non-dimension form

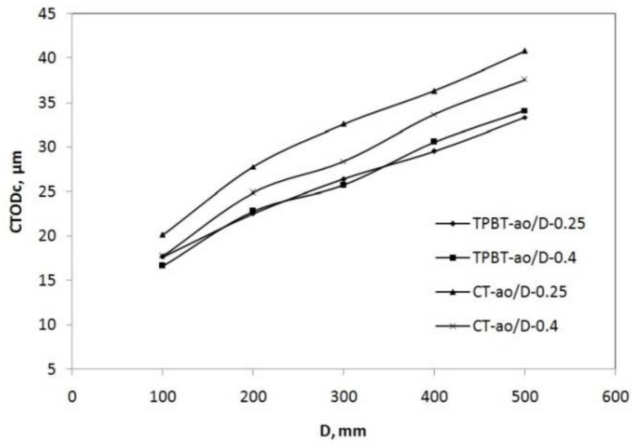

Fig. 9 Variation of CTODc with specimen size

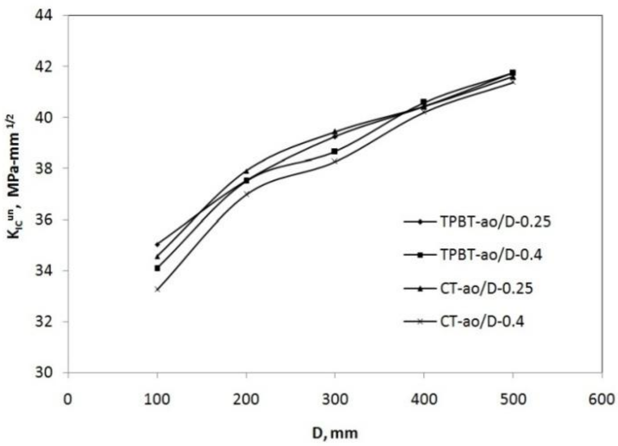

Fig. 10 Variation of unstable fracture toughness with specimen size

value $CMOD_c$ of compact tension specimen is more than those of three point bend test specimen.

Fig. 7 shows the variation of critical value of effective crack length a_c with specimen size. From the figure it is seen that this relationship is linear and it is interesting to observe that the value of effective crack length for both the specimen geometries is almost same and it increases with the specimen size. However, the value of a_c is dependent on the a_o/D ratio. From experimental test results, Zhang and Xu (2011) computed the average value of a_c as 116.94 mm and 172.09 mm for D = 200 mm and 300 mm respectively at a_o/D ratio of 0.4 for wedge splitting specimen. From the numerical result, in the present study, this value of a_c is evaluated as 102.56 mm and 148.17 mm for D = 200 mm and 300 mm respectively at a_o/D ratio for CT specimen whereas these are calculated as 103.39 mm and 149.44 mm for D = 200 mm and 300 mm respectively for TPBT specimen.

The critical effective crack length and specimen size can be expressed in non-dimensional parameters as $(a_c-a_o)/L_{ch}$ and D/L_{ch} respectively where the characteristic length $L_{ch} = EG_F/f_t^2$. These non-dimensional parameters are plotted in Fig. 8, within the size range considered in the study. From the figure, it is observed that $(a_c-a_o)/L_{ch}$ increases with the increase in D/L_{ch}. Similar pattern of the relationship between $(a_c-a_o)/L_{ch}$ and D/L_{ch} was also presented by Zhang and Xu (2011) based on experimental results.

The computed value of $CTOD_c$ versus specimen size is shown in Fig. 9. From the figure it is seen that the value of $CTOD_c$ increases with increase in specimen size. It is also observed that the $CTOD_c$ depends on specimen geometry and a_o/D ratio.

The relationship between K_{IC}^{un} and specimen depth is presented in Fig. 10 which shows a nonlinear increase in the value of K_{IC}^{un} with increase in specimen size up to of 400 mmm. Beyond this value of the specimen size, the value of K_{IC}^{un} is almost independent of specimen geometry and the geometrical factor (a_o/D ratio). Based on experimental test results on wedge splitting specimen, Zhang and Xu (2011) showd that the value of K_{IC}^{un} slightly increases linearly with specimen size.

From Figs. 11-12 it is observed that as compared with Gauss–Chebyshev integral method, the weight function method gives almost the same values of K_{IC}^{C}, the simplified equivalent cohesive force method yields a little different value of K_{IC}^{C} which may not be distinguished from the plots whereas the SGFM yields somewhat different value of K_{IC}^{C}. This deviation in results of K_{IC}^{C} obtained from simplified Green's function method is more for higher value of a_o/D ratio and lower value of specimen depth. The maximum absolute difference in the value of cohesive toughness as compared with Gauss–Chebyshev integral method is 11.62% and 10.9% for TPBT and CT specimen respectively for D = 100 mm at a_o/D ratio of 0.4.

Similarly the relationship between K_{IC}^{ini} obtained using different methods and specimen size for TPBT and CT specimen are shown in Figs. 13 and 14 respectively.

The value of cohesive toughness using four analytical methods: Gauss–Chebyshev integral method, simplified Green's function method, weight function method and simplified equivalent cohesive force method for TPBT and CT specimens are obtained as mentioned in the previous section 3.5. These values are then plotted with specimen size and shown in Figs. 11 and 12 for three point bens test and compact tension specimens respectively. The legends in the figures GCIM, SGFM, WFM and SECFM represent the values obtained using Gauss–Chebyshev integral method, simplified Green's function method, weight function method and simplified equivalent cohesive force method respectively.

From Figs. 13-14 it can be seen that the initiation toughness obtained using weight function method is very close to those obtained using Gauss–Chebyshev integral method. As compared to Gauss–Chebyshev integral method, the simplified equivalent cohesive force method yields initiation toughness with a maximum absolute error of 1.5%. Further simplified Green's function

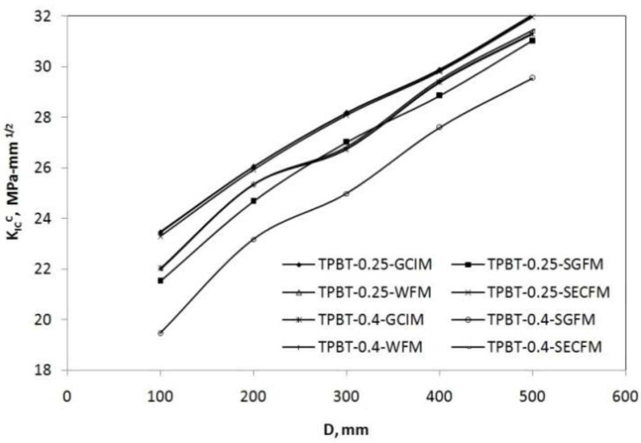

Fig. 11 Variation of cohesive toughness with specimen size for TPBT

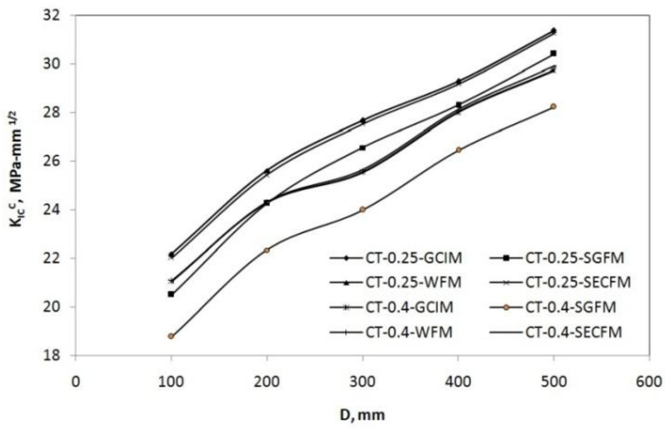

Fig. 12 Variation of cohesive toughness with specimen size for CT specimen

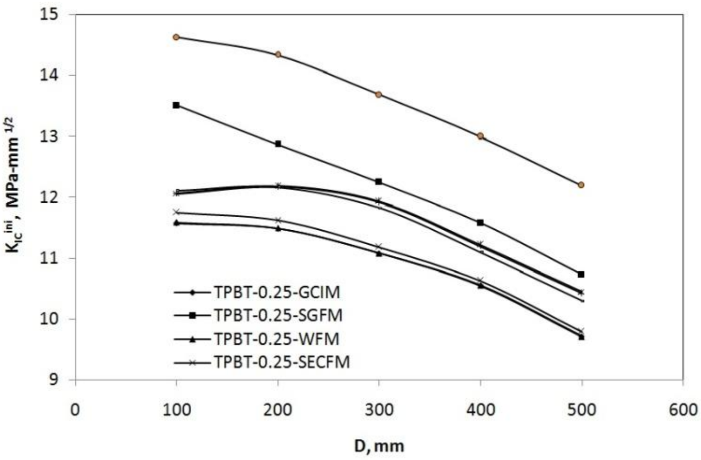

Fig. 13 Variation of initial cracking toughness with specimen size for TPBT

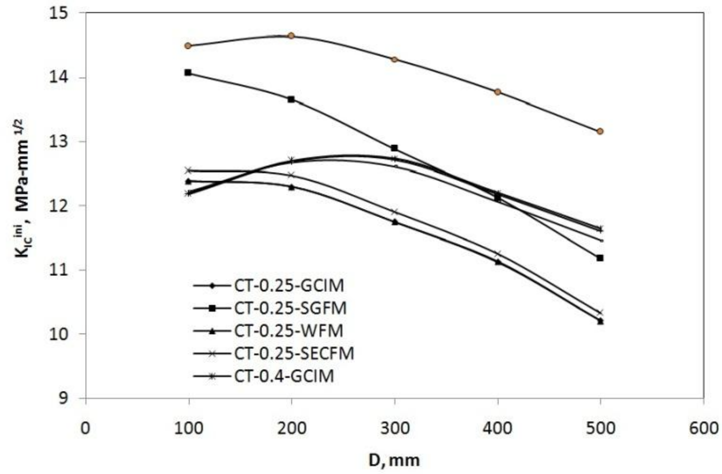

Fig. 14 Variation of initial cracking toughness with specimen size for CT specimen

method yields K_{IC}^{ini} with more error as compared to Gauss–Chebyshev integral method and the maximum absolute error is 21.20% for TPBT and 18.84% for CT specimen for D = 100 mm at a_o/D ratio of 0.4. The formulae presented by Zhang and Xu (2011) has been used in calculation of K_{IC}^{C} using simplified Green's function method for linear stress distribution in the fictitious fracture zone. However, based on experimental test results, Zhang and Xu (2011) reported the maximum variations in these fracture parameters evaluated using these four analytical approaches and the bilinear cohesive stress distribution in the fictitious fracture zone are below 5%.

6. Conclusions

In the present study, a systematic comparison of double-*K* fracture parameters determined using four analytical methods: Gauss–Chebyshev integral method, simplified Green's function method, weight function method and simplified equivalent cohesive force method was carried out on the three point bend test and compact tension test geometries with various specimen sizes (100 – 500 mm) and geometrical factors 0.25 - 0.40). From the study the following concluding remarks can be outlined.

• All the fracture parameters such as critical effective crack length, critical crack tip opening displacement, unstable fracture toughness, cohesive toughness and initial cracking toughness depend on specimen size and geometrical factor. The relationship between effective crack length and specimen size is almost linear and the value of effective crack length increases with the specimen size and is independent of the shape of the specimen.

• The value of unstable fracture toughness increases nonlinearly with increase in specimen size up to of 400 mmm and beyond this value of the specimen size, the value unstable fracture toughness is almost independent of specimen geometry and the geometrical factor.

• The cohesive toughness obtained for linear cohesive stress distribution in the fracture zone using Gauss–Chebyshev integral method, weight function method and simplified equivalent cohesive force method is almost the same while as compared with Gauss–Chebyshev integral method; the simplified Green's function method yields the result with a maximum absolute difference by 11.62%.

• Consequently, the initiation toughness obtained using weight function method is very close to those obtained using Gauss–Chebyshev integral method whereas as compared to Gauss–Chebyshev integral method, the simplified equivalent cohesive force method yields crack initiation toughness with a maximum absolute error of 1.5%. As compared with Gauss–Chebyshev integral method, simplified Green's function method yields the value of initial cracking toughness by the maximum absolute error of 21.20%.

Reference

ASTM International Standard E399-06 (2006), Standard test method for linear-elastic method plane-strain fracture toughness K_{IC} of metallic materials, Copyright ASTM International, West Conshohocken, U.S., 1-32.

Bažant, Z.P. and Oh, B.H. (1983), "Crack band theory for fracture of concrete", *Mater. Struct.*, **16**(93), 155-177.

Bažant, Z.P., Kim, J.K. and Pfeiffer, P.A. (1986), "Determination of fracture properties from size effect tests", *J. Struct. Eng. ASCE*, **112**(2), 289-307.

Carpinteri, A. (1989), "Cusp catastrophe interpretation of fracture instability", *J. Mech. Phy. Solids*, **37**(5), 567-582.

Cusatis, G. and Schauffert, E.A. (2009), "Cohesive crack analysis of size effect", *Eng. Fract. Mech.*,**76**, 2163-2173.

Elices, M., Rocco, C. and Roselló, C. (2009), "Cohesive crack modeling of a simple concrete: Experimental and numerical results", *Eng. Frac. Mech.*, **76**, 1398-1410.

Hillerborg, A., Modeer, M. and Petersson, P.E. (1976), "Analysis of crack formation and crack growth in concrete by means of fracture mechanics and finite elements", *Cement Concrete Res.*, **6**, 773-782.

Hu S. and Lu J. (2012), "Experimental research and analysis on double-*K* fracture parameters of concrete", *Adv. Sci. Lett.*, **12**(1), 192-195.

Hu S., Mi Z. and Lu J. (2012), Effect of crack-depth ratio on double-*K* fracture parameters of reinforced concrete", *Appl. Mech. Mater.*, **226-228**, 937-941.

Jenq, Y.S. and Shah, S.P. (1985), "Two parameter fracture model for concrete", *J. Eng. Mech. ASCE*, **111** (10), 1227-1241.

Kaplan, M.F. (1961), "Crack propagation and the fracture of concrete", *Am. Concrete Inst.*, **58**(5), 1961, 591-610.

Karihaloo, B.L. and Nallathambi, P. (1991), *Notched Beam Test: Mode I Fracture Toughness*, Report of RILEM Technical Committee 89-FMT (Eds. Shah, P. and Carpinteri, A.), Chamman & Hall, London, 1-86.

Kumar, S. and Barai, S.V. (2008a), "Influence of specimen geometry on determination of double-*K* fracture parameters of concrete: A comparative study", *Int. J. Fract.*, **149**, 47-66.

Kumar, S. and Barai, S.V. (2008b), "Cohesive crack model for the study of nonlinear fracture behaviour of concrete", *J. Inst. Engng. (India)*, **89**, 7-15.

Kumar, S. and Barai, S.V. (2009a), "Determining double-*K* fracture parameters of concrete for compact tension and wedge splitting tests using weight function", *Eng. Fract. Mech.*, **76**, 935-948.

Kumar, S. and Barai, S.V. (2009b), "Influence of loading condition and size-effect on the K_R-curve based on the cohesive stress in concrete", *Int. J. Fract.*, **156**, 103-110.

Kumar, S. and Barai, S.V. (2009c), "Effect of softening function on the cohesive crack fracture parameters of concrete CT specimen", *Sadhana-Acad. Proc. Eng. Sci.*, **36**(6), 987-1015.

Kumar, S. and Barai, S.V. (2010a), "Determining the double-*K* fracture parameters for three-point bending notched concrete beams using weight function", *Fatigue Fract. Engng. Mater. Struct.*, **33**(10), 645-660.

Kumar, S. and Barai, S.V. (2010b), "Size-effect prediction from the double-*K* fracture model for notched concrete beam", *Int. J. Damage Mech.*, **19**, 473-497.

Kumar, S. and Pandey, S.R. (2012), "Determination of double-*K* fracture parameters of concrete using split-tension cube test", *Comp. Concr. An Int. J.*, **9**(1), 1-19.

Kwon, S.H., Zhao, Z. and Shah, S.P. (2008), "Effect of specimen size on fracture energy and softening curve of concrete: Part II. Inverse analysis and softening curve", *Cement Concrete Res.*, **38**, 1061-1069.

Murthy, A.R., Iyer N.R. and Prasad B.K.R (2012), "Evaluation of fracture parameters by double-*G*, double-*K* models and crack extension resistance for high strength and ultra high strength concrete beams", *Comput. Mater. Continua.*, **31**(3), 229-252.

Murakami, Y. (1987), *Stress Intensity Factors Hand Book*, Committee on Fracture Mechanics, The Society of Materials Science, Japan Vol-1, Pergamon Press, Oxford.

Nallathambi, P. and Karihaloo, B.L. (1986), "Determination of specimen-size independent fracture toughness of plain concrete", *Mag. Concrete Res.*, **38**(135), 67-76.

Park, K., Paulino, G. H. and Roesler, J.R. (2008), "Determination of the kink point in the bilinear softening model for concrete", *Eng. Frac Mech.*, **7**, 3806-3818.

Petersson, P.E. (1981), *Crack Growth and Development of Fracture Zone in Plain Concrete and Similar Materials*, Report No. TVBM-100, Lund Institute of Technology.

Planas, J. and Elices, M. (1991), "Nonlinear fracture of cohesive material", *Int. J. Fract.*, **51**, 139-157.

Reinhardt, H.W., Cornelissen, H.A.W. and Hordijk, D.A. (1986), "Tensile tests and failure analysis of concrete", *J. Struct. Eng., ASCE*, **112**(11), 2462-2477.

RILEM Draft recommendation (50-FMC) (1985), "Determination of the fracture energy of mortar and concrete by means of three-point bend test on notched beams", *Mater. Struct.*, **18**, 285-290.

RILEM Draft Recommendations (TC89-FMT) (1990), "Determination of fracture parameters (K_{Ic}^{s} and $CTOD_c$) of plain concrete using three-point bend tests", *Mater. Struct.*, **23**(138), 457-460.

Roesler J., Paulino, G.H., Park, K. and Gaedicke, C. (2007), "Concrete fracture prediction using bilinear softening", *Cement Concrete Compos.*, **29**, 300-312.

Tada, H., Paris, P.C. and Irwin, G. (1985), *The Stress Analysis of Cracks Handbook*, Paris Productions Incorporated, St. Louis, Missouri, USA.

Xu, S. and Reinhardt, H.W. (1998), "Crack extension resistance and fracture properties of quasi-brittle materials like concrete based on the complete process of fracture", *Int. J. Fract.* **92**, 71-99.

Xu, S. and Reinhardt, H.W. (1999a), "Determination of double-*K* criterion for crack propagation in quasi-brittle materials, Part I: Experimental investigation of crack propagation", *Int. J. Fract.*, **98**, 111-149.

Xu, S. and Reinhardt, H.W. (1999b), "Determination of double-*K* criterion for crack propagation in quasi-brittle materials, Part II: analytical evaluating and practical measuring methods for three-point bending notched beams", *Int. J. Fract.*, **98**, 151-177.

Xu, S. and Reinhardt, H.W. (1999c), "Determination of double-*K* criterion for crack propagation in quasi-brittle materials, Part III: compact tension specimens and wedge splitting specimens", *Int. J. Fract.*, **98**, 179-193.

Xu, S. and Reinhardt, H.W. (2000), "A simplified method for determining double-*K* fracture meter parameters for three-point bending tests", *Int. J. Fract.*, **104**, 181-209.

Xu, S. and Zhang, X. (2008), "Determination of fracture parameters for crack propagation in concrete using an energy approach", *Engng. Fract. Mech.*, **75**, 4292-4308.

Xu, S. and Zhu, Y. (2009), "Experimental determination of fracture parameters for crack propagation in hardening cement paste and mortar", *Int. J. Fract.*, **157**, 33-43.

Zhang, X., Xu, S. and Zheng, S. (2007), "Experimental measurement of double-*K* fracture parameters of concrete with small-size aggregates", *Front. Archit. Civ. Eng. China*, **1**(4), 448-457.

Zhang, X. and Xu, S. (2011), "A comparative study on five approaches to evaluate double-*K* fracture toughness parameters of concrete and size effect analysis", *Eng. Fract. Mech.*,**78**, 2115-2138.

Zhao, Y. and Xu, S. (2002), "The influence of span/depth ratio on the double-*K* fracture parameters of

concrete", *J China Three Georges Univ.* (*Nat. Sci.*), **24**(1), 35-41.
Zhao, Z., Kwon, S.H. and Shah, S.P. (2008), "Effect of specimen size on fracture energy and softening curve of concrete: Part I. Experiments and fracture energy", *Cement Concrete Res.*, **38**, 1049-1060.
Zi. G. and Bažant, Z.P. (2003), "Eignvalue method for computing size effect of cohesive cracks with residual stress, with application to kink-bands in composites", *Int. J. Eng. Sci.*, **41**, 1519-1534.

CC